

Validation of National Data Buoy Center Directional Wave Measurements Using Swell Waves from Distant Storms

Theodore Mettlach MSMO CCM
Science Application International Corporation
Space, Earth and Atmospheric Sciences Group
National Data Buoy Center Technical Services Contract, Building 3205
Stennis Space Center, Mississippi 39529-6000 USA

Chung-Chu Teng PhD PE
National Data Buoy Center
Building 1100
Stennis Space Center, MS 39529-6000 USA

Abstract-Accuracy of swell wave direction measurements derived from Datawell Hippy 40-second Mark II and National Data Buoy Center angular rate sensor (ARS) are determined using two NDBC west coast stations: 46042 in Monterey Bay and 46028 near Cape San Martin. These are located in deep water 66 nautical miles apart off the central coast of California. Hippy and ARS spectral wave directions are compared to corresponding directions inferred from strong cyclonic wind fields represented by data obtained from National Center for Environmental Prediction/National Center for Atmospheric Research (NCEP/ NCAR) Reanalysis project of NOAA Earth System Research Laboratory (ESRL). Wave energy is assumed to propagate along great circle routes at its frequency-dependent group velocity. Time of wave generation is computed by the ridgeline method. Patterns found in contours of non-directional wave energy on time-frequency plots yield precise information on the time of swell generation. Frequency-dependent wave direction is determined using NDBC techniques. Swell origin position from buoy information is compared to true swell origin, determined to be where high winds exceeding 15 meters per second are found directed toward the station. We present the twelve and only cases from November 2004 to December 2005 in which peak wave period exceeded 20 seconds at NDBC station 46042. In the twelve cases, swell energy reached both stations nearly simultaneously. Storm centers were all deep extra-tropical cyclones, and these ranged across the entire Pacific Ocean. The most distant storm was 3,005 kilometers away in the southern Pacific near 60 degrees south 150 degrees west. Together, these cases show ARS-derived directions marginally exceeding NDBC error limits of 10 degrees. Accuracy of Hippy direction is estimated to be 7 ± 10 degrees. The viability of the validation method as a general technique for any directional wave system is discussed. The last of the twelve cases, the one with the least spectral energy density, representing a wave of period 21 seconds with an amplitude of 13 centimeters, is shown requiring further research owing to apparently weak winds around projected point of swell origin.

I. INTRODUCTION

Vigorous swell waves concern us because of the material effect these have on human activity and economy. Coastal managers and ocean engineers cannot ignore them. The U.S. Army

Corps of Engineers (USACE), having responsibility in monitoring national coastline dynamics, has partnered with NDBC for over two decades in an effort to study the effect of wave action on harbors, beaches and other coastal features. NDBC has deployed several directional wave stations providing long-term records of wave climatology for USACE.

An important aspect of the NDBC wave measurement program is the quality of wave direction estimates, especially of swell waves. It is a straightforward matter characterizing accuracy of higher frequency wave directions. Direction of locally generated, wind waves can be correctly inferred from anemometric measurements, and, if a superstructure vane is installed, from buoy heading. Too, swell wave directions can be approximately checked by comparing these to the location of land and discounting directions giving inadequate fetch. Refraction diagrams can also be used in the same way. But at deep water locations open to a wide sector of directions facing great distances of ocean expanse verifying directional accuracy entails no small effort.

NDBC directional wave estimates are obtained from free floating, moored, discuss buoys. Estimates are based on the slope-following method. Since waves of interest, those having periods beyond one second, exceed in length the diameter of NDBC buoy hulls, it is assumed a buoy follows the surface of the water and that measurements of slope can be used to derive wave characteristics based on linear wave theory. A practical complication arises in measuring long period waves for which amplitudes and slopes can be small. A one-meter high, 20-second period wave slopes up and down one half degree over one wave cycle. Such minuscule, relatively slowly occurring pitch and roll motions can be detected only by higher quality, more responsive sensors.

At present the two primary directional wave sensor systems used by NDBC are, first, the Datawell Hippy 40 and, second, a triaxial angular rate sensor combined with an along-mast accelerometer. The latter system is preferred owing to reduced cost, diminished size, decreased weight and lower electrical

power consumption requirements but only if meeting or exceeding NDBC directional accuracy standards of ± 10 degrees. This paper gives a method for examining accuracy of NDBC wave directions using information from distant storms. Contemporaneous data acquired in three ways are used: (1) from a Datawell Hippy 40-second Mark II sensor on station 46042 in Monterey Bay, California; (2) from an angular rate sensor (ARS) on NDBC station 46028 near Cape San Martin, California; and (3) information from weather analyses provided by National Center for Environmental Prediction/National Center for Atmospheric Research (NCEP/NCAR) Reanalysis project of NOAA Earth System Research Laboratory (ESRL). Buoy wave directions are compared to those from which waves generated by large, faraway distant marine cyclones would propagate.

II. METHODS OF ANALYSIS WITH PITCH-ROLL-HEAVE BUOY

References [1] and [2] give NDBC methods for deriving directional wave parameters with pitch-roll-heave, discus buoys. These methods apply to measurements from both the Hippy and the ARS sensor.

A. Datawell Hippy

From the Hippy sensor, pitch angle, roll angle and heave displacement are read directly. The reference platform for tilt measurements is gravity-stabilized inside an aluminum-magnesium alloy cylindrical can, weighing 36 kg. Pitch and roll angles are determined by the magnetic flux projected onto the reference platform. The magnetic flux is produced from coils fixed inside the sensor. The coils surrounding the platform move with the outer container of the Hippy, and with the buoy, whereas the inner platform inside remains nearly vertical. The accelerometer in the Hippy is a cantilever inside a conducting fluid. Accelerations are proportional to electrical potential at the end of the cantilever, which moves as it accelerates, between two fixed electrodes. The accelerometer assembly is fixed to the inner platform so accelerations are nearly vertical. A high pass filter is applied. The Hippy electronically double integrates acceleration to produce vertical displacement.

B. Angular Rate System

The NDBC ARS sensor is comprised of a single axis Lucas Schaevitz inclinometer, which provides along-mast acceleration and one BEI Systron Donner angular rate sensor fixed along each of the bow, starboard and mast axes of the station. From the rates, pitch and roll angles are computed, as documented in reference [3]. Recognizing buoy pitch angle p and roll angle r can be separated into mean and time-varying components, such that $p(t) = p_0 + p'(t)$ and $r(t) = r_0 + r'(t)$, we write angular rate ω along the bow, starboard and mast-down axes in terms of p , r , buoy azimuth A , and the time derivative of these as follows:

$$\begin{aligned}\omega_1 &= \dot{r} - \dot{A} \sin p \\ \omega_2 &= \dot{p} \cos r + \dot{A} \cos p \sin r \\ \omega_3 &= \dot{A} \cos p \cos r - \dot{p} \sin r\end{aligned}\quad (1)$$

Rearranging and writing (1) in terms of \dot{p} and \dot{r} yields:

$$\begin{aligned}\dot{p} &= \omega_2 \cos r - \omega_3 \sin r \\ \dot{r} &= \omega_1 + (\omega_2 \sin r + \omega_3 \cos r) \tan p\end{aligned}\quad (2)$$

Assuming that mean pitch and roll are approximately zero allows this approximation

$$\begin{aligned}\dot{p}' &\approx \omega_2 \cos r' - \omega_3 \sin r' \\ \dot{r}' &\approx \omega_1 + (\omega_2 \sin r' + \omega_3 \cos r') \tan p'\end{aligned}\quad (3)$$

Reasoning that NDBC discus buoys rarely pitch or roll more than 20 degrees and that the small angle approximation is valid, (3) can be reduced considerably, resulting in a further approximation.

$$\begin{aligned}\dot{p}' &\approx \omega_2 \\ \dot{r}' &\approx \omega_1\end{aligned}\quad (4)$$

The time derivative of pitch and roll in (4) are integrated to obtain an approximation of pitch and roll, which is then entered into (3). Three iterations are needed to obtain a numerical solution in which the differences between the latest and previous estimates of pitch and roll become insignificant. Initial estimates of these are obtained by integrating the angular rates in (4). Equation (4) is used only once. Subsequent estimates are obtained by integrating (3). Integrations are best done with a fast Fourier transform (FFT) routine. A biaxial magnetometer providing magnetic flux density across the bow and starboard of the buoy is used to obtain buoy azimuth.

C. Obtaining Direction from Pitch-Roll-Heave

Once pitch and roll angles are obtained either directly from the Hippy or by computation, buoy slopes in an earth frame of reference are found. East buoy slope Z_x and north buoy slope Z_y are derived as follows:

$$\begin{aligned}Z_x &= \frac{\sin A \sin p}{\cos p} - \frac{\cos A \sin r}{\cos p \cos r} \\ Z_y &= \frac{\cos A \sin p}{\cos p} + \frac{\sin A \sin r}{\cos p \cos r}\end{aligned}\quad (5)$$

These are the first two of three time series records needed for directional wave estimations. Also required is vertical or mast-aligned acceleration a_z .

Letting $S_1 = \text{fft}(a_z)$, $S_2 = \text{fft}(Z_x)$ and $S_3 = \text{fft}(Z_y)$, where $\text{fft}()$ is any FFT routine, the cross-spectra for N points in each time series, sampled at an interval Δt , we have the following:

$$\begin{aligned}C_{ij}^m &= \frac{2\Delta t}{N} (\text{Re}[S_i] \text{Re}[S_j] + \text{Im}[S_i] \text{Im}[S_j]) \quad i, j = [1, 2, 3] \\ Q_{ij}^m &= \frac{2\Delta t}{N} (\text{Im}[S_i] \text{Re}[S_j] - \text{Re}[S_i] \text{Im}[S_j]) \quad i = 1; j = [2, 3]\end{aligned}\quad (6)$$

Depending on configuration, NDBC stations sample for 20 or 40 minutes. Data acquisition for stations 46042 and 46028 involves 4,096 samples over 2,400 seconds each hour.

Reference [4] gives the Fourier representation of the directional wave spectrum:

$$S(f, \theta) = \frac{a_0}{2} + a_1 \cos \theta + b_1 \sin \theta + a_2 \cos 2\theta + b_2 \sin 2\theta \quad (7)$$

in which

$$\begin{aligned} a_0 &= \frac{C_{11}^m}{\omega^4 \pi} & a_1 &= \frac{Q_{12}^m}{\omega^2 k \pi} & a_2 &= \frac{C_{22}^m - C_{33}^m}{k^2 \pi} \\ b_1 &= -\frac{Q_{13}^m}{\omega^2 k \pi} & b_2 &= \frac{2C_{23}^m}{k^2 \pi} \end{aligned} \quad (8)$$

k is wave number and ω is now angular frequency. The Fourier components are used in obtaining wave directions and the spreading functions:

$$\begin{aligned} \theta_1 &= \arctan(b_1, a_1) \\ \theta_2 &= \frac{\arctan(b_2, a_2)}{2}, \end{aligned} \quad (9)$$

$$\begin{aligned} r_1 &= \frac{1}{a_0} (a_1^2 + b_1^2)^{\frac{1}{2}} \\ r_2 &= \frac{1}{a_0} (a_2^2 + b_2^2)^{\frac{1}{2}}. \end{aligned} \quad (10)$$

With ARS, displacement spectrum $C_{11}(f)$ is obtained from the mast acceleration spectrum, which we denote $C_{11}^m(f)$, found first by dividing by angular frequency to the fourth power representing the mathematical relationship to its second derivative, acceleration. Also, a noise correction NC must be applied to prevent spuriously high spectral values on the low end of the spectrum, due to the especially small frequencies there. Finally, a hull transfer function accounts for the response of buoy to water motion.

$$C_{11}(f) = \frac{C_{11}^m(f) - NC(f)}{(2\pi \cdot f)^4 (R^{hH})^2}. \quad (11)$$

III. OBTAINING SWELL DIRECTION WITH RIDGELINE METHOD

The ridgeline method of determining wave direction was first introduced in reference [5]. It is used herein to provide ground truth for long period swell wave measurements from the two NDBC stations.

A wave of frequency f travels at group speed,

$$C_g(f) = \frac{g}{4\pi \cdot f}. \quad (12)$$

Gravity is g .

In this study we are particularly interested in waves with periods of over 20 seconds. In the second panel of Figure 1, we see a sharp jump in peak period T_p to over 20 seconds occurring near 1000 UTC 18 February at the Monterey station. The buoy to the south measured the same, but a little later at 1600 UTC. The figure also gives time series of significant wave height H_{mo} , average wave period T_{avg} and the direction from which peak wave energy is coming, relative to north, $\alpha_{1p} = 270^\circ - \theta_{1p}$.

From reference [6] we find that dispersion theory describes energy peaks associated with swell waves produce a slanting ridge appearing as a straight line through contours of spectral energy density on a time-frequency plot. The intersection of the ridgeline with the $f = 0$ line will give t_o the time of swell generation. The onset of swell can be identified by a particular spectral energy density threshold at a frequency f at arrival time t_a .

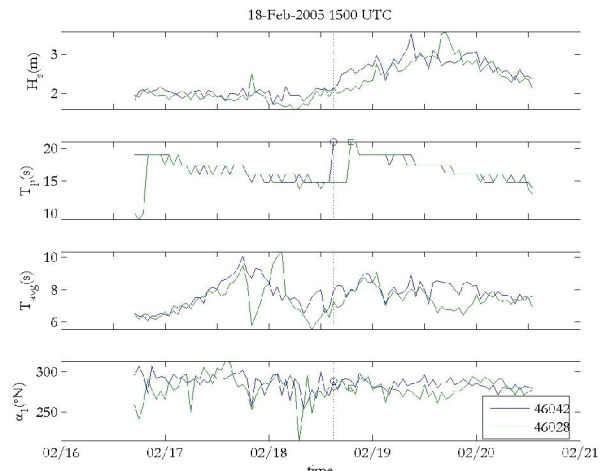


Figure 1. Swell arriving at both stations on 18 February 2005 as noted by peak wave period T_p exceeding 20 seconds in the second panel.

Figure 2 gives an example a ridgeline plot, showing swell originated at time t_o 1200 UTC 18 February, arriving four days later at time t_a on the 22nd, after which wave frequency steadily increased for the next three days.

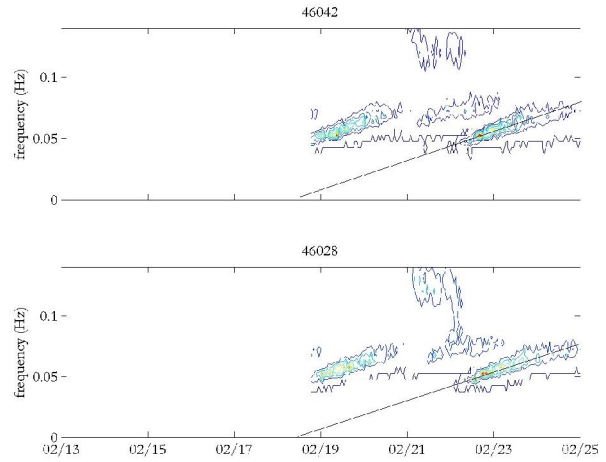


Figure 2. Swell arriving at both stations on 22 February 2005. Contours are of spectral energy density C_{11} , same colors representing in both panels same energy. Red denotes peak energy. Data void on left of plot intentional.

Travel distance d_o is easily computed since wave speed is constant:

$$d_o = C_g(t_a - t_o) \quad (13)$$

After distance from station to origin is computed, weather maps near in time to t_o are inspected for areas of high winds

with sufficient fetch at distance d_o . An example is given in Fig. 3 where wind vectors have been plotted every two and one-half degrees in latitude and longitude. Red arrows denote wind exceeding 15 meters per second, which is gale force, capable of generating moderate to high sea states depending on the fetch and duration. In this figure also are shown the estimated swell generation locations from the two stations in blue for 46042 and red for 46028. Magenta triangle denotes true swell generation location based on the wind pattern.

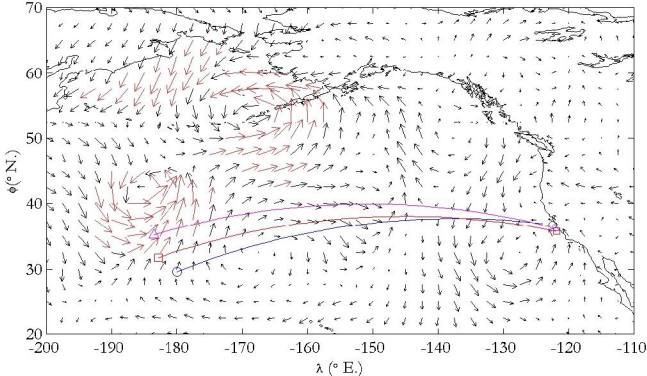


Figure 3. Swell arriving 1200 UTC 18 February 2005. In blue is Hippy estimate. Red is ARS estimate. In magenta color is true swell path.

Finding the estimated point of swell origin $O(\phi_o, \lambda_o)$ requires geographic position of the station $P(\phi_1, \lambda_1)$, peak wave direction α_{1p} and radial distance from station to storm δ_o . Using one degree of arc length for 60 nautical miles, the corresponding angular distance δ_o is computed from d_o . Peak wave direction α_{1p} is obtained from the station using data from Hippy or ARS, as in the fourth panel of Fig. 1. For a station at latitude ϕ_1 longitude λ_1 , $O(\phi_o, \lambda_o)$ is computed with equations (14) and (15).

$$\phi_o = \arcsin(\sin \phi_1 \cos \delta_o + \cos \phi_1 \sin \delta_o \cos \alpha_{1p}) \quad (14)$$

$$\lambda_o = \lambda_1 + \arctan\left(\frac{\sin \delta_o \sin \alpha_{1p}}{\cos \phi_1 \cos \delta_o - \sin \phi_1 \sin \delta_o \cos \alpha_{1p}}\right) \quad (15)$$

IV. DATA SELECTION

Data from stations 46042 Monterey and 46028 Cape San Martin covering 14 months from 15 October 2004 to 15 December 2005 were extracted from the NDBC database. Both stations are standard, aluminum, NDBC 3-meter discus buoys in deep water with identical data acquisition periods and GOES transmission time. Depth at 46042 is 1,920 meters, at 46028, 1,112 m. The stations are separated by 66 nautical miles. Time series data arrays were produced for significant wave height, peak wave period, average wave period, displacement spectrum C_{11} , frequency-dependent wave direction α_I and the first spreading parameter r_I among other things. Hourly frames of data were produced only for those hours in which all data—wave, spectra, spreading functions—were available from both stations.

From 9,846 hours of data there were 53 hours at station 46042 and 60 hours at station 46028 in which peak wave period exceeded 20 seconds. Analysis of the occurrences allowed grouping them into 12 cases. Twelve in one year is not unusual for the eastern Pacific wherein occurrence of long-period swell waves is the result of energetic tropical and extra-tropical cyclones developing throughout the Pacific Ocean throughout the year.

Each case begins with a sharp jump in peak period from well below 20 seconds to 21.1 seconds or 23.5 seconds, after which periods gradually decline somewhat linearly. Only the first jump is used for computing swell generation time, although the arrival time of any particular frequency along the ridgeline could have been used.

V. RESULTS

Eleven of the 12 cases were complete in the sense that meteorological data verified the existence of a distant, prior storm in the vicinity where at least one of the NDBC stations pointed, more or less correctly. Table I summarizes the buoy measurements and ridgeline analysis results of these. Table II lists the differences between bearings of station-derived swell generation locations to those obtained from map analysis. We see that average Hippy-derived wave directions meet the NDBC standard of 10 degrees but that the deviation about the mean error exceeds this slightly. ARS-derived directions clearly exceed those from the Hippy although in some particular cases the ARS proved to be the more accurate system. The tenth case was of the most distant storm near 60 degrees south latitude, where the closest land was Antarctica. ARS pointed over 40 degrees too far left looking out from the station, and there is no obvious reason for this error. Hippy always pointed to within 22 degrees of true wave direction.

The last of the 12 cases is extremely interesting because of the apparent lack of any storms anywhere that might have generated the swell signal detected by both stations, and in much the same way. Fig. 4 gives a detail of the area suggested by the buoy data to have been where the swell had originated. South of the Philippines there is seen a weak cyclonic circulation but nothing strong. A search for tropical systems in the area revealed no activity. However, a closer look at the data in Table III suggests a possible answer to this mystery. The wave amplitude $a(f)$ associated with the spectral energy of a component of the wave spectrum C_{11} is found by the following relationship.

$$a(f) = \sqrt{2C_{11}\Delta f} \quad (16)$$

Table III lists the amplitudes of 23.5- and 21-second wave energy first detected by the respective station for each case. We see that the amplitudes for Case 12 are least from among the whole set of 12 cases, giving a reasonable explanation for why a storm could not be found. A short-lived, small-scale weather event likely created the swell energy but this event was too small to have been integrated into the NCAR reanalysis fields, of which there are only four fields per day and which are mapped to a coarse 2.5 by 2.5-degree grid. Nevertheless small swell waves propagated away from the origina-

tion site, reaching the West Coast of the U.S. several days later.

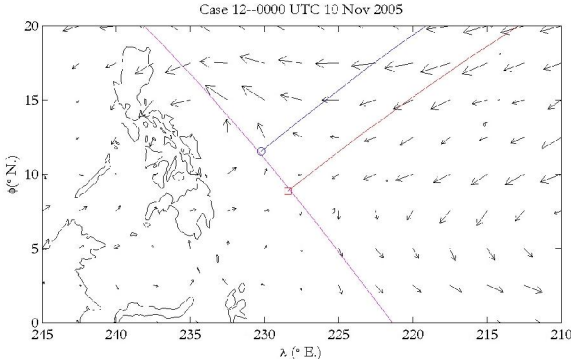


Figure 4. Detail of wind pattern around estimated swell origin positions for case 12. Blue circle and curve give swell origin point and swell propagation path from Hippy data. In red is the same, except for ARS. Magenta curve is segment of a circle centered between the two buoys of radius d_o .

TABLE I

SUMMARY OF CASES GIVING MEASURED PEAK WAVE PERIOD, WAVE DIRECTION AND HOURS OF WAVE PROPAGATION DETERMINED FROM RIDGELINE.

Case No.	Date of swell arrival	46042			46028		
		T_p sec	α_p deg	t_a-t_0 hours	T_p sec	α_p deg	t_a-t_0 hours
1	16 Dec 2004	21.05	286	108	21.05	267	109
2	23 Dec 2004	19.05	285	139	21.05	270	137
3	3 Jan 2005	21.05	310	133	23.53	300	133
4	18 Jan 2005	21.05	293	111	21.05	261	112
5	16 Feb 2005	21.05	284	134	19.05	291	140
6	18 Feb 2005	21.05	288	93	21.05	280	97
7	22 Feb 2005	21.05	279	90	21.05	284	94
8	1 Mar 2005	23.53	276	83	21.05	277	87
9	9 Mar 2005	21.05	291	100	21.05	294	100
10	15 Sep 2005	21.05	196	185	21.05	157	186
11	23 Oct 2005	21.05	304	43	23.53	293	46
12	17 Nov 2005	21.05	290	182	21.05	287	184

We speculate that the source of the average error in the ARS sensor is lack of sensitivity to minuscule rotational rates associated with the small slopes of swell waves. This stems from the relatively small mass of the sensor which remains uncoupled to the complementary data available from the mast accelerometer. Source of error in the Hippy is attributed to the known limitations resulting from rapid changes in azimuth.

TABLE II
SUMMARY OF TRUE WAVE DIRECTIONS DERIVED FROM METEOROLOGICAL WIND FIELDS AND DEPARTURE OF STATION REPORTS FROM THESE. BELOW ARE BASIC STATISTICS OF THE ERRORS BY STATION.

Case No.	True wave direction (degrees N.)	46042 error (degrees)	46028 error (degrees)
1	305	-19	-38
2	299	-14	-29
3	299	11	1
4	293	0	-31
5	300	-16	-9
6	292	-4	-12
7	288	-9	-4
8	298	-22	-21
9	294	-3	0
10	198	-2	-41
11	299	5	-6
12	--	--	--
Mean error		-6.6	-17.3
Standard deviation of error		10.3	15.4
Maximum error		11.0	1.0
Minimum error		-22.0	-41.0
Error range		33.0	42.0

TABLE III
AMPLITUDE IN METERS ASSOCIATED WITH MEASURED SPECTRAL ENERGY DENSITY AT TWO FREQUENCIES BY CASE BY STATION.

Case No.	46042		46028	
	.0425 Hz	.0475 Hz	.0425 Hz	.0475 Hz
1	0.03	0.21	0.04	0.17
2	0.04	0.26	0	0.25
3	0.32	0.15	0.25	0.15
4	0	0.18	0	0.22
5	0	0.20	0	0.14
6	0.11	0.36	0.07	0.46
7	0.15	0.35	0.10	0.42
8	0.33	0.17	0.18	0.78
9	0.21	0.45	0.31	0.45
10	0.15	0.16	0.07	0.17
11	0.18	0.20	0.32	0.39
12	0.05	0.13	0.07	0.10

VI. DISCUSSION

Storms produce winds that generate waves, which travel from their generation area along great circle routes. These waves can often progress thousands of miles before crashing or breaking against the coast. The physical characteristics of these is to be of relatively small-amplitude, to have long-period and to travel rapidly. Owing to distance from origin station bearing to the generation area can be determined accurately and precisely using well accepted, well proven, elementary, linear wave theory governing the propagation of deep water waves. Applying these, we have evaluated the characteristic accuracy of the Datawell Hippy 40 and the NDBC ARS on the standard NDBC 3-meter discus buoy.

There is little doubt that the Hippy 40 is the superior sensor but we should be surprised that, in general, its performance is near the limit of acceptability by NDBC and USACE. Contin-

ued improvement in the NDBC waves program shall demand a focused examination of the complete hull-mooring-sensor system.

Limitation of the ARS system is illustrated well by large errors in four of the 11 cases. Each of these produced large negative errors with which we should discount random effects of some kind. Wave-current interaction may be the key to understanding these seemingly systematic errors.

NDBC is slowly perfecting ways to measure swell waves. The ridgeline method is one of the least expensive validation tools available as development of swell-measuring techniques continues. Wind wave direction can be corroborated with wind direction from two anemometers. Swell wave direction is not as simple to check, although there are two ways. First, there is the orientation of the coast, from which swell cannot come. If a station is near land then a gross check of wave direction is possible. Also, other sensors, such as arrays of pressure gages, can be used. Accurate *in situ* validation systems are expensive, bulky, cumbersome and difficult to maintain. Therefore, the ridgeline method has a place at NDBC because it is accurate and simple, easy to understand and straightforward, and it is interesting to learn.

Using cases in which the peak wave period exceeded 20 seconds was done with a purpose. It was to find what might be termed *clean* cases, relatively uncomplicated by energies associated with other frequencies of the wave spectrum. An unexpected consequence of this selection criterion was to give us cases with relatively small wave amplitudes, and, thus diminished wave slopes, which we have shown were effectively detected by both the Hippy and ARS. The high sensitivity of the ARS sensors to mild-sloping waves has encouraged continued development and application of micro-electro-mechanical motion sensor technology. Presently NDBC has adapted the MicroStrain gyro-enhanced orientation sensor 3DM-GX1 to replace the Schaevitz-Systron Donner assembly.

Case 12 invites more discussion and a closer look for two reasons. First, it demonstrates the magnifying effect of stacking ridgelines. This increases the signal to noise ratio considerably, bringing out subtle features. The same occurs with $\alpha_1(f)$ when true, yet weak, signals arrive at a buoy. Methods for signal detection based on continuity in times series was not examined in this report but such an examination could open up some doors into the world of intelligent post-processing of data. Second, Case 12 establishes the importance of wave analysis as a new method for tracking the existence of storms at sea. What we may have discovered here is a method for tracking short-lived, far-off wind events that may have slipped through the meteorological reporting grid. If so, this has implications in climate-energy balance studies because we will have demonstrated a method for tracking small-scale, energetic meteorological phenomena as reflected in the ocean wave field.

ACKNOWLEDGEMENT

This work was done under the general NDBC technical services contract with Science Application International Corporation, Space, Earth and Scientific Applications Group. NCEP Reanalysis data provided by the NOAA/OAR/ESRL PSD, Boulder, CO USA from their website at www.cdc.noaa.gov.

REFERENCES

- [1] Steele, K. E., Joseph Chi-Kin Lau and Yuan-Huang L. Hsu, "Theory and application of calibration techniques for an NDBC directional wave measurements buoy", *IEEE J. Ocean. Engeng.*, **OE-10** (4), pp. 382-396, 1985.
- [2] Steele, K. E., Chung-Chu Teng and D.W.C. Wang, "Wave direction measurements using pitch-roll buoys", *Ocean Engeng.*, **19**(4), 349-375, 1992
- [3] Steele, K. E., D. W. Wang, M. D. Earle, E. D. Michelena and R.J. Dagnall, "Buoy pitch and roll computed using three angular rate sensors," *Coast. Eng.*, **35**, 123-139, 1998.
- [4] Longuet-Higgins, M. S., D. E. Cartwright and N.D. Smith, "Observations of the directional spectrum of sea waves using the motions of a floating buoy", *Ocean Wave Spectra*, pp. 111-136, 1963
- [5] Munk, W. H., G. R. Miller, F. E. Snodgrass and N. F. Barber, "Directional recording of swell from distant storms," *Phil. Trans. Roy. Soc. London*, **A255**, 505-584, 1963.
- [6] Mettlauch, Theodore, David Wang and Paul Wittmann, "Analysis and Prediction of Ocean Swell using Instrumented Buoys," *J. Atmos Ocean. Tech*, **11**(2), 506-524, 1994.